Acta Cryst. (1997). A53, 556–563

Modelling Electrostatic Potential from Experimentally Determined Charge Densities. II. Total Potential

NOUZHA BOUHMAIDA,[a] NOUR-EDDINE GHERMANI,[b] CLAUDE LECOMTE[b]* AND ABDELMALEK THALAL[a]

[a]*Laboratoire des Sciences des Matériaux, Université Cadi Ayyad, Faculté des Sciences Semlalia, BP S15, 40000 Marrakech, Morocco, and* [b]*Laboratoire de Cristallographie et Modélisation des Matériaux Minéraux et Biologiques, LCM3B, URA CNRS 809, Université Henri Poincaré, Nancy 1, Faculté des Sciences, Boulevard des Aiguillettes, BP 239, 54506 Vandoeuvre-lès-Nancy CEDEX, France. E-mail: lecomte@lcm3b.u-nancy.fr*

(*Received 2 November 1996; accepted 14 March 1997*)

Abstract

Experimental electrostatic potential derived from X-ray diffraction data was used as a given physical property for the determination of atomic moments. The electrostatic potential is fitted against Buckingham moments expansion up to octupolar level. The estimation of the contribution of the aspherical part of the density to the electrostatic potential necessitates a judicious choice of the points grid around the system in order to get stability and reliability of the results. The net charges obtained by the fit to the electrostatic potential on a test crystal of the pseudo-peptide *N*-acetyl-α,β-dehydrophenylalanine methylamide are close to those derived from the electron-density refinements. The higher moments are related to the electron-density multipolar parameters.

1. Introduction

In molecular modelling and molecular dynamic simulations, the charge-density distribution cannot be used directly from theory or experiment. It should be parametrized: in a first approximation, it can be represented by a simple superposition of net charges centred at atomic sites. This representation has two advantages: firstly, it allows the electrostatic interaction of the molecule to be described easily; secondly, these net atomic charges determined on small molecules are supposed to be intrinsic for atoms in some fragments and then could be transferable to similar fragments of larger systems for which the density distribution is nearly impossible to reach with accuracy.

The determination of net atomic charges from the molecular electron density necessitates a space partitioning, for example stockholder partitioning (Hirshfeld, 1977), discrete boundary (Moss & Coppens, 1981) or topological analysis of Bader (Bader & Nguyen-Dand, 1981; Bader, 1990) to define the real occupied atomic volume in the whole molecule. These charges are obtained by direct integration of the electron density on the atomic volumes. However, this method suffers from serious numerical difficulties especially on the volume boundaries and also because the charge density of outer atoms extends formally to infinity. All methods define also very different atomic volumes and different integrated charges.

The second and more convenient approach to obtain the charges is based on fitting to a basic physical property like the electrostatic potential or electric field derived either from quantum-mechanical calculations (Momany, 1978; Cox & Williams, 1981; Chirlian & Francl, 1987) or from the experiment. The point charges positioned on the nuclei can reproduce accurately the electrostatic potential when it is generated by the spherical part of the electron density or from a κ refinement (Ghermani, Bouhmaida & Lecomte, 1993, paper I) or if the potential is calculated far from the charge distribution. This latter case is obviously not interesting since the interaction between molecules occurs at a distance corresponding to the molecular van der Waals surface. Moreover, the introduction of the contribution of the aspherical part of the electron density is more than necessary in modelling the electrostatic potential mainly for organic compounds displaying *s*, *p* bonds, lone pairs and hydrogen bridges. When this modelling is based on a point-charge model, sophisticated observation grid-point sampling (Spackman, 1996) or dipole constraint (when experimental values are available) (Woods, Khalil, Pell, Moffat & Smith, 1990) must be used in the fitting procedure in order to get reliable and non-conformational-dependent charge density (Bouhmaida, 1993; Ghermani, Bouhmaida & Lecomte, 1993). Furthermore, once the grid sampling is adequate, in the theoretical case these charges are strictly dependent upon the basis sets used in the calculation of the electrostatic potential. As reported by Woods *et al.* (1990), for methanol (CH_3OH), the atomic charge on the O atom varies from -0.482 e for the STO-3G basis set to -0.682 e for 6-31G** wavefunction potential. This latter value was also found by Spackman (1996) with his geodesic sampling points using 6-31G** wavefunction; the atomic charges of the methyl group, which are more sensitive to the polarization effect, are, however, different from those of Woods *et al.* (1990).

Another way to improve the fit of the electrostatic potential by point charges consists of adding extra-nucleus centres, for example charges in the middle of

the bonds in amino acid side chains (Chipot, Angyan, Maigret & Sheraga, 1993). The number of centres will obviously increase with the size of the molecule and the physical significance of these charges will be doubtful. In fact, this multicentring representation of the electrostatic potential is mathematically equivalent to a multipolar expansion on atomic sites. Faerman & Price (1990) have shown that this latter representation yields more accurate electrostatic potential at all distances from the atoms and a better estimation of the interaction energy than a point-charge model.

On the other hand, our experimental approach is based on the accurate electron density derived from high-resolution X-ray diffraction data. In the refinement of the electron density, the molecular electron distribution is considered as a superposition of multipolar pseudo-atoms. Since the diffraction data are due to interacting molecules in the crystal, the multipolar density parameters are supposed to contain much more information than in the isolated molecule, especially for features like hydrogen bonds. At the end of an experimental electron-density study, the electrostatic potential can be calculated analytically with respect to the multipolar density parameters (Ghermani, Lecomte & Bouhmaida, 1993). In paper I, we have obtained reliable charges by fitting the electrostatic potential calculated from the spherical density contribution using the Householder method (Lascaux & Theodor, 1986). The charges obtained were very close to those obtained from X-ray analysis and were not found to be conformation dependent. Other studies on the determination of point charges are those of Su & Coppens (1993) and Klooster & Craven (1992). We have also shown in paper I that the determination of charges from the total electrostatic potential, *i.e.* including the aspherical part of the electron density, was not possible with good accuracy because of the difficulty in the representation of this asphericity by atomic site point charges. The aim of this second paper is to show that chemically realistic atomic moments can be determined from a least-squares fit to the total electrostatic potential (in this paper, experimental potential). These moments will also be compared with the charge-density multipolar parameters.

2. Methodology

Our experimental X-ray diffraction data are refined using a multipolar model (Hansen & Coppens, 1978) in which the electron density of each atom in the molecule is given by

$$\rho(\mathbf{r}) = \rho_{\text{core}}(r) + P_{\text{val}}\kappa'^3\rho_{\text{val}}(\kappa r) + \sum_l \kappa''^3 R_{nl}(\kappa'' r)\sum_m P_{lm} y_{lm\pm}(\theta,\varphi), \quad (1)$$

where ρ_{core} and ρ_{val} are, respectively, Hartree–Fock spherical core and valence densities, ρ_{val} is normalized to 1 e; then the refined valence population parameter P_{val} gives the net atomic charge q with respect to the number of electrons N_{val} in the free-atom valence orbitals, $q = N_{\text{val}} - P_{\text{val}}$. The $y_{lm\pm}$'s are spherical harmonic angular functions of order l in real form and $R_{nl}(r)$ are Slater-type radial functions

$$R_{nl}(r) = N_l r^{nl}\exp(-\zeta r). \quad (2)$$

N_l is the normalization factor, nl and ζ are parameters depending on the atomic type. P_{lm} are the multipolar population parameters and κ' and κ'' are contraction–expansion coefficients for spherical and multipolar valence densities, respectively. The molecular density is considered as the superposition of the pseudo-atomic densities. It is then possible, from the analytical expression of the electron density, to calculate the atomic moments with respect to the Hansen–Coppens model parameters. Many studies on dipole moments derived from experimental X-ray diffraction were done [see for example those of Coppens, Guru Row, Leung, Stevens, Becker & Yang (1979) or more recently the study of Espinosa, Lecomte, Molins, Veintemillas, Cousson & Paulus (1996)]; the results are comparable with other experiment or quantum-mechanical results. Moss & Feil (1981) have also calculated higher atomic moments directly from the Hirshfeld charge-density model (Hirshfeld, 1971). Our approach is to consider the electrostatic potential as a given physical property that can be attained from experiment or calculated (instead of the charge density) to derive atomic moments; the electrostatic potential compares better than electron density from one method to another, mainly outside the charge distribution (van der Waals envelope). This was confirmed recently by the comparison between *ab initio* SCF and experimental electrostatic potential in the hydrogen-bond region of a nonlinear optical (NLO) material L-arginine phosphate monohydrate (LAP) (Espinosa, Lecomte, Ghermani *et al.*, 1996). Fitting atomic moments against electrostatic potential seems therefore to be more suitable to compare the results from theoretical or experimental strategies.

We have shown that the molecular electrostatic potential (Ghermani, Lecomte & Bouhmaida, 1993) is the sum of the contributions of each atom j at $\mathbf{R}_j$:

$$V(\mathbf{r}) = \sum_j V_{j\,\text{core}}(r) + V_{j\,\text{val}}(r) + \Delta V_j(\mathbf{r})$$

with

$$V_{j\,\text{core}}(r) = \frac{Z_j}{|\mathbf{r}-\mathbf{R}_j|} - \int \frac{\rho_{j\,\text{core}}(r')}{|\mathbf{r}-\mathbf{R}_j-\mathbf{r}'|}\,\mathrm{d}^3\mathbf{r}',$$

$$V_{j\,\text{val}}(r) = -\int P_{\text{val}_j}\kappa_j'^3 \frac{\rho_{j\,\text{val}}(\kappa_j' r')}{|\mathbf{r}-\mathbf{R}_j-\mathbf{r}'|}\,\mathrm{d}^3\mathbf{r}' \quad (3)$$

and

$$\Delta V_j(\mathbf{r}) = -4\pi \sum_{lm}[\kappa_j'' P_{jlm}/(2l+1)] \times \Bigg([1/(\kappa_j''^{l+1}|\mathbf{r}-\mathbf{R}_j|^{l+1})] \times \int_0^{\kappa_j''|\mathbf{r}-\mathbf{R}_j|} t^{l+2} R_{jnl}(t)\,dt + \kappa_j''^{l}|\mathbf{r}-\mathbf{R}_j|^{l} \times \int_{\kappa_j''|\mathbf{r}-\mathbf{R}_j|}^{\infty} [R_{jnl}(t)\,dt/t^{l-1}] \Bigg) y_{lm\pm}(\theta', \varphi'). \quad (4)$$

In our previous study (paper I), we have shown that the electrostatic potential calculated from the spherical part of the charge density related to Z, ρ_{core} and ρ_{val} could be fitted beyond a radius $|\mathbf{r}-\mathbf{R}|_{\min} = 2$ Å by point charges on the nuclear positions. This point-charge fitting was performed on several thousands of observation points equally distributed on a spherical grid around each atom, the minimum distance $|\mathbf{r}-\mathbf{R}|_{\min}$ being 2 Å. The values obtained are close to net atomic charges deduced from P_{val} and are not conformation dependent. We also understood, in this paper, that increasing the number of observation points does not change significantly the results.

The fit of the contribution, to the electrostatic potential, of the aspherical part of the density by q/R is difficult since the multipolar functions could not be described by a single point charge on each nucleus and it is necessary at least to add supplementary centres or dipoles on hydrogen atoms (Bouhmaida, 1993). Hence, the fit with point charges of the total potential gives a statistical residual factor $R_{\%}$ defined by $R_{\%} = (\sum_i^{N_{\text{obs}}} |V_{\text{obs}\,i} - V_{\text{calc}\,i}|^2 / \sum_i^{N_{\text{obs}}} V_{\text{obs}\,i}^2)^{1/2}$ greater than 30% when this factor is less than 1% for the spherical density contribution. Therefore, in this study, the fit of the experimental electrostatic potential was then carried out using the Buckingham (1959) atomic moments expansion up to octupolar level ($l = 3$) given by

$$V(\mathbf{r}) = \sum_j \sum_{lm} (Q_{jlm}/|\mathbf{r}-\mathbf{R}_j|^{l+1}) y_{lm\pm}(\theta', \varphi'), \quad (5)$$

where Q_{jlm} represents the m moment of order l of the atom j in the molecule, $|\mathbf{r}-\mathbf{R}_j|$ being the distance between the observation point at $\mathbf{r}$ and the atom j at $\mathbf{R}_j$.

3. Sampling scheme

3.1. *Choice of the minimum distance*

The fit to the aspherical multipolar part of the electrostatic potential requires a careful study of the sampling observation points since these multipolar functions contribute mainly in particular directions of the space. In the interatomic region, the atomic moments Q_{jlm} depend upon the distance as shown by Vigné-Maeder & Clavérie (1988). Furthermore, the distance must be greater than 2 Å because at about 2 Å from the atoms the polarization and exchange effects become negligeable. On the other hand, the magnitude of the higher multipolar functions are important in the region close to the atoms ($d < 1$ Å) compared with the contribution of the monopole. Then we must find a suitable limit of the distance from each atom $|\mathbf{r}-\mathbf{R}|_{\min}$ to be used in the fit. For this, consider the ratio of the radial parts in the potential between (4) and (5), namely the function

$$\left[\int_0^{|\mathbf{r}-\mathbf{R}_j|} t^{l+2} R_{jnl}(t)\,dt\right] + \left[|\mathbf{r}-\mathbf{R}_j|^{2l+1} \int_{|\mathbf{r}-\mathbf{R}_j|}^{\infty} R_{jnl}(t)\,dt/t^{l-1}\right], \quad (6)$$

which is represented as a function of r in Fig. 1 for an O atom with $\zeta = 4.5$, $\kappa'' = 1$, $l = 2$ and $nl = 2$. Fig. 1 shows that this function becomes constant at an average distance of 2 Å; this distance was then taken as the minimal value in the fit. The curves obtained for C, N and H atoms show similar features.

3.2. *Choice of the sampling scheme*

Consider a fragment of four atoms as shown in Fig. 2, which displays the sampling observation spheres. The observation points are chosen equidistant on spheres centred on the nuclear positions. In the previous study, the points were sampled only on the external van der Waals-like envelop (heavy line in Fig. 2). This choice gives very small weight to the inner atoms in the molecule whose charges and moments may not be well determined (ill conditioning problem); therefore, the sampling points are chosen on spheres centred on all the atoms (radius = 2 Å) with the condition that the potential at a given point M is calculated and fitted with only the contribution of atoms at $|\mathbf{r}-\mathbf{R}_j| > 2$ Å. For illustration, the potential at point M is calculated

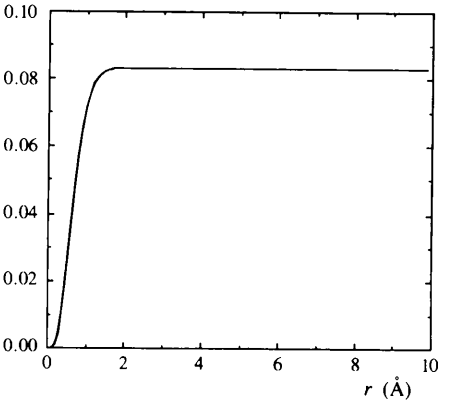

Fig. 1. Ratio of the radial part of the electrostatic potential [formula (6)] for an O atom as a function of the distance r to the atomic centre.

and fitted without atom J contribution ($|\mathbf{r} - \mathbf{R}_j| < 2$ Å) and $V(M) = V_I + V_K + V_L$, where I, K and L relate to the neighbouring atoms. Consequently, on the sphere around a given atom, there are different sectors where the contributors (atoms) are not the same. With this potential rejection criteria, we have almost the same number of sampling points for each atom in the molecule. The fit of the experimental electrostatic potential using the Buckingham atomic moments expansion [formula (5)] was added in our Fortran program *ELECTROS* (Ghermani, Bouhmaida & Lecomte, 1992), which is available on request. In order to avoid ill conditioned least-squares matrices, the Householder resolution method (Lascaux & Theodor, 1986) described in paper I was also applied in the determination of the atomic moments. In order to take into account the chemical and the local symmetry of each atom in the molecule, the calculation is performed in atomic local frames as is usually done in the refinement of the electron density in the Hansen–Coppens (1978) model. This procedure also permits one to describe the electrostatic potential only by significant moments of the atoms imposed by symmetry or pseudo-symmetry of the local atomic sites.

4. Application to *N*-acetyl-α,β-dehydrophenylalanine methylamide

In order to test the improvement of the fit of the total electrostatic potential using the introduction of higher moments on the atoms, the same pseudo-peptide molecule *N*-acetyl-α,β-dehydrophenylalanine methylamide (hereafter AcΔ) (Souhassou *et al.*, 1992) was chosen as in paper I. Fig. 3 shows the *ORTEP* view of AcΔ. During the least-squares *Molly* refinement (Souhassou *et al.*, 1992), we imposed chemical and symmetry constraints on P_{val} and P_{lm} parameters [see formula (1)] like C6 = C7 = C8 = C9 = C10 or H112 = H212 = H312, which are, *de facto*, included in our experimental potential. We will show that our algorithm and sampling points' choice will recover exactly the constrained charges and moments even though we did not impose any constraint in the fit. This fit was performed with one shell of observation points of radius equal to 2 Å around the atoms in the molecular crystalline conformation. We have checked that using more than one shell did not change the results. This is expected because homothetic shells do not change the main directions and thus the contributions to the moments. Table 1 gives the obtained charges and moments up to order $l = 3$ (octupoles) for C, O and N atoms and $l = 1$ (dipoles) for H atoms. The statistical R_{σ} value is very low ($R_{\sigma} = 3.8\%$, $N_{obs} = 12\,210$, $N_{par} = 284$), reflecting the excellent quality of the fit. Fig. 4 displays the experimental potential (*a*) and the electrostatic potential calculated with the obtained atomic moments (*b*). The difference of these maps does not exceed 0.05 e Å^{-1} outside an atomic radius of 1 Å.

4.1. *Net atomic charges*

As shown in Table 1, the net atomic charges are equal within 0.01 e to those given by $N_{val} - P_{val}$ [for-

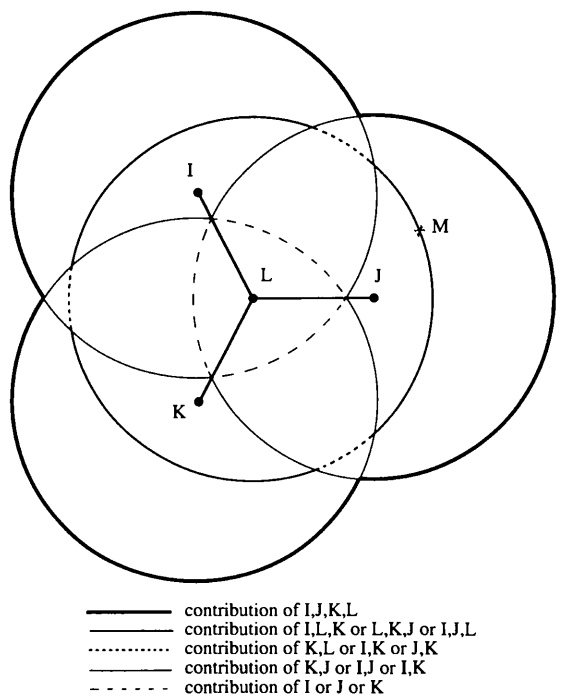

Fig. 2. Example of the observation points sampling grid.

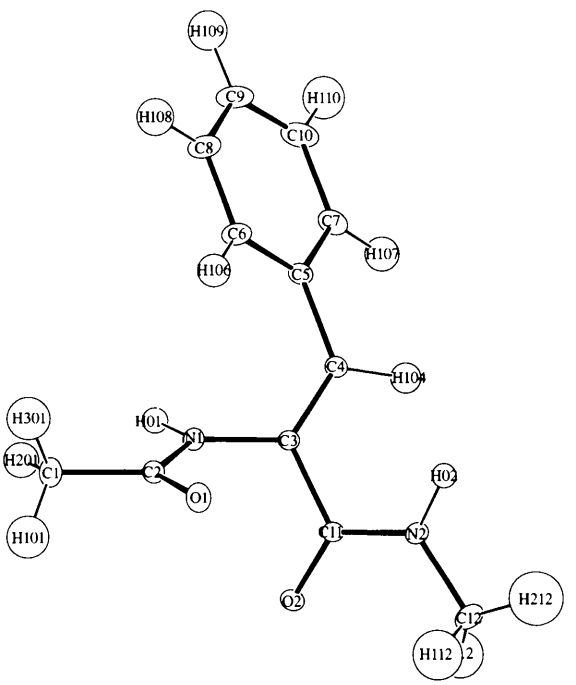

Fig. 3. *ORTEP* view of *N*-acetyl-α,β-dehydrophenylalanine methylamide (AcΔ).

mula (1)]. It is worth noting that, although we did not use any electroneutrality constraint, the total molecular charge remains zero within 0.01 e. This result could be attributed to the good choice of the sampling points, which takes into account in the same way all the atoms of the molecule whatever their positions (inner or outer atoms). This was not exactly the case in paper I, where we found a deviation of approximately 0.2 e from the neutrality for this 30-atom molecule. Furthermore, the net charges obtained in this study are very close to those of the previous paper, the maximal deviation being 0.06 e for the O atoms. They respect symmetry and chemical properties – *i.e.* equivalent atoms have equal charges without constraints. Also, the introduction of the aspherical part does not change the charges. Inspection of the higher atomic moments shows also directly the chemically equivalent atoms. All these remarks show the stability in the Householder resolution.

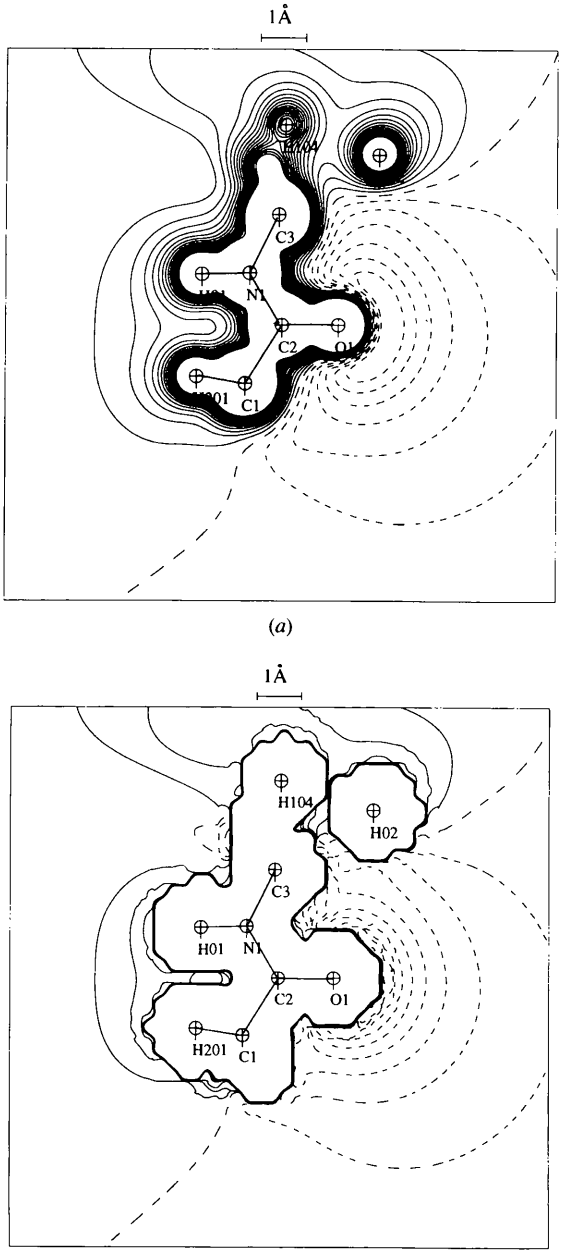

Fig. 4. Electrostatic potential in AcΔ in the plane of a peptide bond. Contours are 0.05 e Å^{-1}, zero and negative contours are dashed: (*a*) experimental electrostatic potential; (*b*) electrostatic potential calculated with the full set of fitted atomic moments.

4.2. *Higher atomic moments*

For the chemically equivalent and constrained atoms in the multipolar density refinements, the obtained atomic moments in their local atomic frames are almost equal; see, for example, the phenyl C atoms (C6, C7, C8, C9, C10) and their corresponding H atoms (Table 1). Furthermore, in the phenyl group, for instance, only the moments corresponding to dipole (x), quadrupole ($3z^2-1$) and octupole ($x^3 - 3xy^2$) have significant values in comparison with the other moments: without any constraint in the fit, these latter results are in accordance with the local atomic symmetry. Hence, the fit of the electrostatic potential could be performed with a restricted number of moments: it was therefore done with only the moments that gave a minimal contribution of 0.02 e Å^{-1} to $V(r)$ at a distance of 2 Å from the atomic centres. This reduced the number of parameters from 284 to 132. The statistical $R_{\%}$ factor is 4.3% compared with 3.8% in the unconstrained fit. Table 2 gives the results obtained when the total potential is fitted with this restricted set of parameters. They agree almost exactly with the statistically significant moments of the full parameters fit, the highest deviation being 0.04 e Å^3 for the octupole ($x^3 - 3xy^2$) of C1. This observation also enhances the robustness of the method, showing that the main components are very well determined, not depending on the number of parameters. The electrostatic potential map calculated with the restricted set of moments is quasi-exactly superposable on the map obtained with the full set (see supplementary material).*

5. Relationship between the atomic moments and the multipole density parameters

In the experimental approach, the molecular electron density is projected onto pseudo-atom densities described by products of radial terms with spherical harmonic functions in real form. The P_{lm} parameters of each of these pseudo-atoms contain information related to the bonding and the interaction between molecules

* A figure showing the electrostatic potential in AcΔ calculated with the reduced set of fitted atomic moments has been deposited with the IUCr. Copies may be obtained through The Managing Editor, International Union of Crystallography, 5 Abbey Square, Chester CH1 2HU, England (Reference: AU0091).

Table 1. *Atomic moments (in e Å^l, l is the multipolar level) obtained in the fit to experimental electrostatic potential of AcΔ with the full set of parameters*

Spherical harmonics functions are given in their Cartesian form related to x, y, z. The local axis frame is given in Souhassou *et al.* (1992).

Atom	P_{val}	Charge (e)	X	Y	Z	X^2-Y^2	XY	XZ	YZ	$3Z^2-1$	X^3-3XY^2	$3X^2Y-Y^3$	ZX^2-ZY^2	XYZ	$(5Z^2-1)X$	$(5Z^2-1)Y$	$5(Z^2-3)Z$
C1	4.25	−0.24	0.24	−0.20	−0.01	0.37	0.12	0.01	−0.03	−0.24	−0.97	0.27	−0.17	0.10	1.08	0.71	−0.24
C2	3.87	0.14	−0.49	−0.28	0.17	−0.28	0.07	0.05	−0.07	0.90	−1.44	0.04	−0.02	0.04	0.17	0.04	−0.04
C3	4.10	−0.09	−0.64	−0.35	0.24	−0.35	0.14	0.07	0.04	0.35	−0.96	−0.09	0.03	−0.03	−0.14	−0.15	0.16
C4	3.88	0.13	−0.03	−0.18	−0.21	−0.02	0.02	0.02	−0.07	0.45	−1.19	0.09	0.03	0.16	−0.23	−0.14	−0.06
C5	4.02	−0.01	0.10	−0.02	−0.02	0.11	−0.01	−0.03	0.04	0.67	1.21	0.04	0.00	0.08	−0.15	−0.02	0.05
C6	4.10	−0.09	−0.12	−0.02	0.00	0.01	0.00	0.01	−0.01	0.54	1.07	0.04	−0.04	−0.02	−0.07	0.04	0.03
C7	4.10	−0.09	−0.11	0.00	0.00	0.04	0.01	−0.03	−0.02	0.54	1.10	−0.01	−0.03	−0.01	−0.01	0.01	0.03
C8	4.10	−0.09	−0.13	0.01	0.01	0.03	0.02	0.03	−0.03	0.55	1.10	0.02	−0.01	0.01	−0.07	0.01	0.00
C9	4.10	−0.09	−0.12	0.00	0.00	0.01	−0.02	0.00	−0.01	0.58	1.06	0.04	0.00	0.03	−0.03	0.01	0.02
C10	4.10	−0.09	−0.12	0.00	0.00	−0.02	0.01	−0.01	0.00	0.60	1.10	−0.02	0.03	0.00	−0.04	0.00	0.02
C11	4.10	−0.09	−0.35	0.22	0.01	−0.22	0.06	0.07	0.04	0.86	−1.52	0.08	−0.01	0.14	0.03	−0.06	0.06
C12	4.32	−0.31	0.68	0.46	−0.08	0.24	−0.03	−0.09	−0.12	−0.29	−1.64	−0.30	0.17	0.20	1.44	−0.27	−0.12
O1	6.37	−0.38	0.26	−0.13	−0.15	0.01	−0.07	0.03	0.04	0.07	−0.03	−0.05	0.02	0.00	−0.03	0.05	0.00
O2	6.44	−0.44	0.22	−0.02	−0.01	0.05	−0.03	0.00	0.03	0.10	0.04	−0.02	−0.03	−0.03	0.00	−0.01	0.02
N1	5.31	−0.30	−0.19	−0.23	0.08	0.00	0.04	−0.03	0.01	0.06	−0.58	−0.03	−0.01	−0.16	−0.10	0.00	0.01
N2	5.08	−0.08	0.02	−0.29	0.09	0.08	0.06	−0.02	0.08	0.03	−0.51	0.06	−0.02	−0.03	0.06	0.03	−0.09
H101	0.87	0.13	−0.62	—	—	—	—	—	—	—	—	—	—	—	—	—	—
H201	0.87	0.13	−0.60	—	—	—	—	—	—	—	—	—	—	—	—	—	—
H301	0.87	0.13	−0.63	—	—	—	—	—	—	—	—	—	—	—	—	—	—
H104	0.84	0.15	−0.52	—	—	—	—	—	—	—	—	—	—	—	—	—	—
H106	0.84	0.15	−0.52	—	—	—	—	—	—	—	—	—	—	—	—	—	—
H107	0.84	0.15	−0.51	—	—	—	—	—	—	—	—	—	—	—	—	—	—
H108	0.84	0.15	−0.51	—	—	—	—	—	—	—	—	—	—	—	—	—	—
H109	0.84	0.15	−0.53	—	—	—	—	—	—	—	—	—	—	—	—	—	—
H110	0.84	0.15	−0.52	—	—	—	—	—	—	—	—	—	—	—	—	—	—
H112	0.87	0.13	−0.63	—	—	—	—	—	—	—	—	—	—	—	—	—	—
H212	0.87	0.13	−0.63	—	—	—	—	—	—	—	—	—	—	—	—	—	—
H312	0.87	0.13	−0.58	—	—	—	—	—	—	—	—	—	—	—	—	—	—
H01	0.75	0.24	−0.52	—	—	—	—	—	—	—	—	—	—	—	—	—	—
H02	0.76	0.23	−0.74	—	—	—	—	—	—	—	—	—	—	—	—	—	—

in the solid state. Now, if we take any pseudo-atom and compare (4) and (5), it is obvious that at a great distance from the nucleus site, *i.e.* outside the atomic density distribution, P_{lm} will be proportional to Q_{lm} as pointed out by Vigné-Maeder & Clavérie (1988) for $Q_{lm}(R)$ and $Q_{lm}(\infty)$. In this study, we calculate directly the atomic moments with respect to the molecular electrostatic potential, which is a function of the total electron density everywhere in the space. Then the obtained atomic moments Q_{jlm} have to be compared with the multipolar density parameters P_{jlm}. The ratios $Q_{jlm}/4\pi P_{jlm}\Phi_{jl}(\infty)$ are listed in Table 3, where $\Phi_{jl}(\infty)$ is the value of the first integral in (6) (the second part converges to 0):

$$\Phi_{jl}(\infty) = \lim_{|\mathbf{r}-\mathbf{R}_j|\to\infty} \int_0^{|\mathbf{r}-\mathbf{R}_j|} t^{l+2} R_{jnl}(t)\, dt. \qquad (7)$$

In practice, this integral is constant when $|\mathbf{r} - \mathbf{R}_j| = 30$ Å). We note that this ratio is l independent, which is not the case for Φ_{jl}.

As shown in Table 3, these ratios are close to 1.0 for atoms like phenyl C atoms, which are described by only a net charge, one dipole, one quadrupole and one octupole ($0.9 <$ ratio < 1.12). The same remark holds for H atoms ($0.8 <$ ratio < 1.04). For other atoms of the molecule, these ratios are very different from 1.0 even if the number of statistically significant moments is low. In the case of O and N atoms, the values of Q_{lm} can be three times those of P_{lm}. Describing the methyl C atoms is more complex because they require at least 12 moments and the resulting ratios exceed 2.0. These preliminary results show that the ratios are related to the type of fragment the atom belongs to and its environment. We are currently applying the method to other molecular compounds and testing the transferability of atomic moments and their use in modelling. This study will complement the work of Pichon-Pesme, Lecomte & Lachekar (1995) concerning the transferability of the P_{lm} electron-density parameters.

6. Conclusions

The total electrostatic potential including spherical and aspherical density contributions is fitted by atomic moments following the Buckingham expansion up to octupolar level for organic molecules. The new sampling of the observation points proposed here yields reliable results and permits unequivocal decorrelation between the net charges related to the spherical density on one hand and the higher atomic moments on the other hand.

Table 2. *Atomic moments (in e Å^l, l is the multipolar level) in the fit to experimental electrostatic potential of AcΔ with the reduced set of parameters*

Atom	P_{val}	Charge (e)	X	Y	Z	X^2-Y^2	XY	XZ	YZ	$3Z^2-1$	X^3-3XY^2	$3X^2Y-Y^3$	ZX^2-ZY^2	XYZ	$(5Z^2-1)X$	$(5Z^2-1)Y$	$5(Z^2-3)Z$
C1	4.25	−0.24	0.26	−0.20	—	0.36	0.12	—	—	−0.24	−1.01	0.26	−0.16	0.12	1.11	0.71	−0.19
C2	3.87	0.14	−0.48	−0.30	0.17	−0.32	—	—	—	0.93	−1.44	—	—	—	0.20	—	—
C3	4.10	−0.09	−0.63	−0.32	0.29	−0.35	0.14	—	—	0.31	−0.95	—	—	—	−0.15	−0.12	0.21
C4	3.88	0.13	—	−0.15	−0.25	—	—	—	—	0.40	−1.20	—	—	0.06	−0.31	−0.12	—
C5	4.02	−0.01	0.10	—	—	0.08	—	—	—	0.63	1.18	—	—	—	−0.19	—	—
C6	4.10	−0.09	−0.12	—	—	—	—	—	—	0.54	1.11	—	—	—	—	—	—
C7	4.10	−0.09	−0.11	—	—	—	—	—	—	0.56	1.10	—	—	—	—	—	—
C8	4.10	−0.09	−0.14	—	—	—	—	—	—	0.58	1.08	—	—	—	—	—	—
C9	4.10	−0.09	−0.14	—	—	—	—	—	—	0.60	1.07	—	—	—	—	—	—
C10	4.10	−0.09	−0.13	—	—	—	—	—	—	0.59	1.13	—	—	—	—	—	—
C11	4.10	−0.09	−0.32	0.23	—	−0.19	—	—	—	0.88	−1.43	—	—	0.18	—	—	—
C12	4.32	−0.31	0.69	0.44	—	0.24	—	−0.10	—	−0.29	−1.64	−0.28	0.15	0.20	1.41	−0.32	−0.09
O1	6.37	−0.38	0.27	−0.13	−0.15	—	—	—	—	—	—	—	—	—	—	—	—
O2	6.44	−0.44	0.22	—	—	—	—	—	—	0.10	—	—	—	—	—	—	—
N1	5.31	−0.30	−0.23	−0.24	—	—	—	—	—	—	−0.52	—	—	−0.14	−0.10	—	—
N2	5.08	−0.08	—	−0.29	—	—	—	—	—	—	−0.48	—	—	—	—	—	−0.12
H101	0.87	0.13	−0.61	—	—	—	—	—	—	—	—	—	—	—	—	—	—
H201	0.87	0.13	−0.59	—	—	—	—	—	—	—	—	—	—	—	—	—	—
H301	0.87	0.13	−0.65	—	—	—	—	—	—	—	—	—	—	—	—	—	—
H104	0.84	0.15	−0.54	—	—	—	—	—	—	—	—	—	—	—	—	—	—
H106	0.84	0.15	−0.53	—	—	—	—	—	—	—	—	—	—	—	—	—	—
H107	0.84	0.15	−0.53	—	—	—	—	—	—	—	—	—	—	—	—	—	—
H108	0.84	0.15	−0.49	—	—	—	—	—	—	—	—	—	—	—	—	—	—
H109	0.84	0.15	−0.53	—	—	—	—	—	—	—	—	—	—	—	—	—	—
H110	0.84	0.15	−0.52	—	—	—	—	—	—	—	—	—	—	—	—	—	—
H112	0.87	0.13	−0.62	—	—	—	—	—	—	—	—	—	—	—	—	—	—
H212	0.87	0.12	−0.62	—	—	—	—	—	—	—	—	—	—	—	—	—	—
H312	0.87	0.13	−0.61	—	—	—	—	—	—	—	—	—	—	—	—	—	—
H01	0.75	0.24	−0.50	—	—	—	—	—	—	—	—	—	—	—	—	—	—
H02	0.76	0.23	−0.71	—	—	—	—	—	—	—	—	—	—	—	—	—	—

Table 3. *Ratios $Q_{jlm}/4\pi P_{jlm}\Phi_{jl}(\infty)$ of atom j, where Q_{lm} are the atomic moments and P_{lm} the multipolar electron density parameters; $\Phi_{jl}(\infty)$ is the value of the first integral in formula (6)*

Atom	X	Y	Z	X^2-Y^2	XY	XZ	YZ	$3Z^2-1$	X^3-3XY^2	$3X^2Y-Y^3$	ZX^2-ZY^2	XYZ	$(5Z^2-1)X$	$(5Z^2-1)Y$	$5(Z^2-3)Z$
C1	1.51	1.10	—	2.16	1.20	—	—	2.06	1.34	−0.96	2.50	1.46	1.28	1.12	2.15
C2	1.00	1.48	1.12	1.27	—	—	—	1.23	1.10	—	—	—	1.23	—	—
C3	1.10	0.94	1.25	1.43	1.70	—	—	0.79	0.90	—	—	—	0.74	0.72	7.82
C4	—	2.47	1.61	—	—	—	—	0.88	1.13	—	—	0.53	1.28	1.44	0.59
C5	1.17	—	—	0.81	—	—	—	1.13	1.09	—	—	—	1.22	—	—
C6	0.96	—	—	—	—	—	—	0.99	1.02	—	—	—	—	—	—
C7	0.93	—	—	—	—	—	—	1.03	1.01	—	—	—	—	—	—
C8	1.11	—	—	—	—	—	—	1.06	0.99	—	—	—	—	—	—
C9	1.12	—	—	—	—	—	—	1.11	0.98	—	—	—	—	—	—
C10	1.05	—	—	—	—	—	—	1.10	1.04	—	—	—	—	—	—
C11	1.03	1.48	—	0.85	—	—	—	1.20	1.01	—	—	1.71	—	—	—
C12	1.24	1.08	—	6.51	—	1.15	—	1.92	1.38	−1.28	0.57	1.41	1.23	1.95	5.47
O1	1.25	1.71	1.38	—	—	—	—	—	—	—	—	—	—	—	—
O2	1.39	—	—	—	—	—	—	1.46	—	—	—	—	—	—	—
N1	1.47	1.58	—	—	—	—	—	—	1.23	—	—	2.43	2.04	—	—
N2	—	1.07	—	—	—	—	—	—	1.39	—	—	—	—	—	3.43
H101	0.92	—	—	—	—	—	—	—	—	—	—	—	—	—	—
H201	0.89	—	—	—	—	—	—	—	—	—	—	—	—	—	—
H301	0.97	—	—	—	—	—	—	—	—	—	—	—	—	—	—
H104	1.00	—	—	—	—	—	—	—	—	—	—	—	—	—	—
H106	0.98	—	—	—	—	—	—	—	—	—	—	—	—	—	—
H107	0.98	—	—	—	—	—	—	—	—	—	—	—	—	—	—
H108	0.91	—	—	—	—	—	—	—	—	—	—	—	—	—	—
H109	0.97	—	—	—	—	—	—	—	—	—	—	—	—	—	—
H110	0.96	—	—	—	—	—	—	—	—	—	—	—	—	—	—
H112	0.94	—	—	—	—	—	—	—	—	—	—	—	—	—	—
H212	0.93	—	—	—	—	—	—	—	—	—	—	—	—	—	—
H312	0.92	—	—	—	—	—	—	—	—	—	—	—	—	—	—
H01	0.83	—	—	—	—	—	—	—	—	—	—	—	—	—	—
H02	1.04	—	—	—	—	—	—	—	—	—	—	—	—	—	—

The net charges are very close to those derived from the electron-density refinement, namely $q = N_{val} - P_{val}$; this shows that our algorithm is very well conditioned. Also, charges and moments for symmetry or chemically equivalent atoms are almost equal. With respect to the local atomic symmetry, some of the moments are not significant and could be excluded in the fit to the total electrostatic potential. This is in favour of including only these significant parameters in molecular modelling. The comparison between the observed potential and the potential calculated with the significant atomic moments only is excellent in the external region of the molecule. Application of the method to several other organic molecules with both experimental and theoretical potentials is in progress.

The support of the CNRS, the CNR (through grant no SPM/3375, 1996), Université Henri Poincaré (Nancy, France) and Université Cadi Ayyad (Marrakech, Morocco) are gratefully acknowledged.

References

Bader, R. F. W. (1990). In *Atoms in Molecules – a Quantum Theory*. Oxford University Press.

Bader, R. F. W. & Nguyen-Dand, T. T. (1981). *Adv. Quantum Chem.* **14**, 63–124.

Bouhmaida, N. (1993). PhD thesis, Université de Nancy 1, France.

Buckingham, A. D. (1959). *Q. Rev. Chem. Soc.* **13**, 183–214.

Chipot, C., Angyan, J. G., Maigret, B. & Sheraga, H. A. (1993). *J. Phys. Chem.* **97**, 9788–9796.

Chirlian, L. E. & Francl, M. M. (1987). *J. Comput. Chem.* **8**, 6, 894–905.

Coppens, P., Guru Row, T. N., Leung, P., Stevens, E. D., Becker, P. & Yang, Y. W. (1979). *Acta Cryst.* A**35**, 63–72.

Cox, S. R. & Williams, D. E. (1981). *J. Comput. Chem.* **2**, 304–323.

Espinosa, E., Lecomte, C., Ghermani, N. E., Devémy, J., Rohmer, M., Bénard, M. & Molins, E. (1996). *J. Am. Chem. Soc.* **118**, 2501–2502.

Espinosa, E., Lecomte, C., Molins, E., Veintemillas, S., Cousson, A. & Paulus, W. (1996). *Acta Cryst.* B**52**, 519–534.

Faerman, C. H. & Price, S. L. (1990). *J. Am. Chem. Soc.* **112**, 4915–4926.

Ghermani, N. E., Bouhmaida, N. & Lecomte, C. (1992). *ELECTROS: Computer Programs to Calculate Electrostatic Properties from High Resolution X-ray Diffraction*. Internal Report URA CNRS 809, Université Henri Poincaré, Nancy 1, France.

Ghermani, N. E., Bouhmaida, N. & Lecomte, C. (1993). *Acta Cryst* A**49**, 781–789.

Ghermani, N. E., Lecomte, C. & Bouhmaida, N. (1993). *Z. Naturforsch. Teil A*, **48**, 91–98.

Hansen, N. K. & Coppens, P. (1978). *Acta Cryst.* A**34**, 909–921.

Hirshfeld, F. L. (1971). *Acta Cryst.* B**27**, 769–781.

Hirshfeld, F. L. (1977). *Theor. Chem. Acta*, **44**, 129–138.

Klooster, W. T. & Craven, B. M. (1992). *Biopolymers*, **32**, 1141–1154.

Lascaux, P. & Theodor, R. (1986). *Analyse Numérique Matricielle Appliquée à l'Art de l'Ingénieur*, Vol. I. Paris: Masson.

Momany, F. A. (1978). *J. Phys. Chem.* **82**, 592–601.

Moss, G. & Coppens, P. (1981). *Chemical Application of Atomic and Molecular Potentials*, edited by P. Politzer & D. G. Truhlar, pp. 427–443. New York: Plenum Press.

Moss, G. & Feil, D. (1981). *Acta Cryst.* A**37**, 414–421.

Pichon-Pesme, V., Lecomte, C. & Lachekar, H. (1995). *J. Phys. Chem.* **99**, 6242–6250.

Souhassou, M., Lecomte, C., Ghermani, N. E., Rohmer, M. M., Wiest, R., Benard, M., Blessing, R. H. (1992). *J. Am. Chem. Soc.* **114**, 2371–2382.

Spackman, M. A. (1996). *J. Comput. Chem.* **17**, 1–18.

Su, Z. & Coppens, P. (1993). *Z. Naturforsch. Teil A*, **48**, 85–90.

Vigné-Maeder, F. & Clavérie, P. (1988). *J. Chem. Phys.* **88**, 4934–4950.

Woods, R. J., Khalil, M., Pell, W., Moffat, S. H. & Smith, V. H. (1990). *J. Comput. Chem.* **11**, 3, 297-319.